



LAWRENCE
LIVERMORE
NATIONAL
LABORATORY

Understanding the implications of the data from recent high-energy-density Kelvin-Helmholtz shear layer experiments

O. A. Hurricane, J. F. Hansen, E. C. Harding, R. P. Drake, H. F. Robey, B. A. Remington, C. C. Kuranz, M. J. Grosskopf, R. S. Gillespie, H. Park

October 27, 2009

The Sixth International Conference on Inertial Fusion Sciences & Applications

San Francisco, CA, United States

September 6, 2009 through September 11, 2009

Disclaimer

This document was prepared as an account of work sponsored by an agency of the United States government. Neither the United States government nor Lawrence Livermore National Security, LLC, nor any of their employees makes any warranty, expressed or implied, or assumes any legal liability or responsibility for the accuracy, completeness, or usefulness of any information, apparatus, product, or process disclosed, or represents that its use would not infringe privately owned rights. Reference herein to any specific commercial product, process, or service by trade name, trademark, manufacturer, or otherwise does not necessarily constitute or imply its endorsement, recommendation, or favoring by the United States government or Lawrence Livermore National Security, LLC. The views and opinions of authors expressed herein do not necessarily state or reflect those of the United States government or Lawrence Livermore National Security, LLC, and shall not be used for advertising or product endorsement purposes.

Understanding the implications of the data from recent high-energy-density Kelvin-Helmholtz shear layer experiments

O.A. Hurricane¹, J.F. Hansen¹, E.C. Harding², R.P. Drake², H.F. Robey¹, B.A. Remington¹, C.C. Kuran², M.J. Grosskopf², R.S. Gillespie², and H. Park¹

¹Lawrence Livermore National Laboratory, 7000 East Avenue, Livermore, CA 94550, USA

²Department of Atmospheric, Oceanic, and Space Sciences, University of Michigan, 2455 Hayward St., Ann Arbor, Michigan 48109-2143, USA

E-mail: hurricane1@llnl.gov

Abstract. The first successful high energy density Kelvin-Helmholtz (KH) shear layer experiments (O.A. Hurricane, et al., Phys. Plasmas, **16**, 056305, 2009; E.C. Harding, et al., Phys. Rev. Lett., **103**, 045005, 2009) demonstrated the ability to design and field a target that produces an array of large diagnosable KH vortices in a controlled fashion. Data from these experiments vividly showed the complete evolution of large distinct eddies, from formation to apparent turbulent break-up. Unexpectedly, low-density bubbles/cavities comparable to the vortex size ($\sim 300 - 400 \mu\text{m}$) appeared to grow up in the free-stream flow above the unstable material interface. In this paper, the basic principles of the experiment will be discussed, the data reviewed, and the progress on understanding the origin of the above bubble structures through theory and simulation will be reported on. (IFSA 1.10.096)

1. Introduction

In May 2009, our team fielded the first successful high-energy-density-physics (HEDP) Kelvin-Helmholtz (KH) experiments [1, 2] on the Omega laser at the University of Rochester. These experiments proved out the unique conceptual design [3] that relied upon shock driven baroclinic vorticity production and also showed that vivid high quality data (see Fig. 1) could be obtained on KH in a HEDP environment.

The basic configuration consists of a stack of opaque high density plastic and low density foam all of which is contained in a shock tube of rectangular cross-section, made from Be so as to be able to radiograph through it with x-rays of a few keV energy (see Fig. 2) – details of the target design can be found in [1]. Laser energy (4 kJ in a 1 ns pulse for this case) is delivered to an 820 μm diameter spot on an ablator covering the low density foam part of the target (on the left of Fig. 2). In this way, a strong shock is launched into the low density foam such that the pressure gradient at the leading edge of the shock would essentially be at right angles to the density gradient at the interface of the two dissimilar materials thus maximizing $\nabla P \times \nabla \rho$. The interface between the two materials is perturbed by a sinusoidal contour with amplitude ($a = 30\mu\text{m}$) and wavelength ($\lambda = 400\mu\text{m}$) chosen such that a number of large vortices would develop nonlinear structure in the expected field of view during the experiment. By in large,

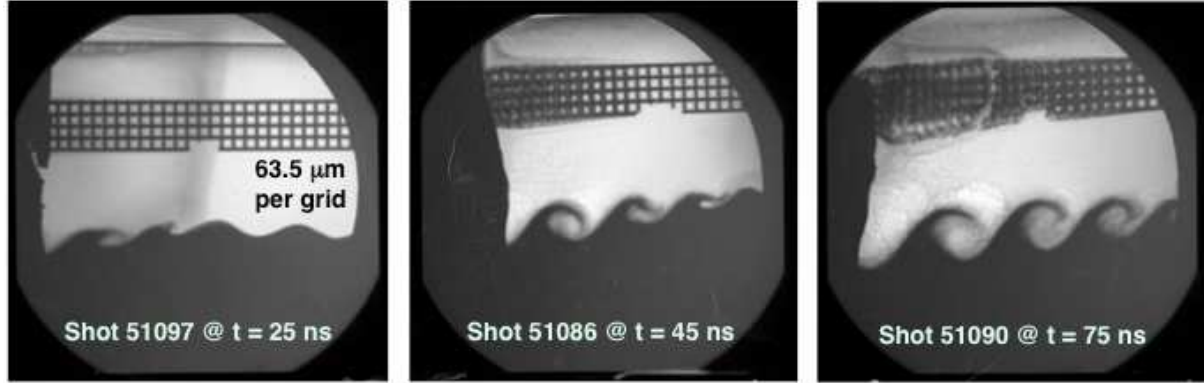


Figure 1. From left to right, radiographic data from Omega shots 51097, 51086, and 51090 are shown. These three images show the time development of the KH instability at 25 ns, 45 ns, and 75 ns respectively. In the left frame, the vorticity producing shock wave is visible in the low density (100 mg/cc) carbon foam. Wave crest begin to develop immediately after passage of the shock wave and grow into full blown vortices (middle frame). At late time (right frame), the spiral arms of the vortices appear to begin to diffuse away presumably the result of turbulence onset.

the data from our May 2008 experiments were consistent with expectations based upon two-dimensional (2D) simulation using the CALE [4] code.

2. Instability Growth

The images shown in Fig. 1 are simply converted into datum of vortex height versus time [2] that can be compared with simulation and theory. In Fig. 3 an updated comparison of the vortex height data is shown against a revised simulation result and theory. The data shown in Fig. 3 are identical to those shown in References [1, 2], but the simulation result shown here superceeds that presented previously. Here the simulation used to produce the data shown in Fig. 3 has been corrected to include the actual as-shot Be shock tube thickness of 500 μ m rather than the 200 μ m thickness used for the simulations shown in [1, 2] and a more accurate method of determining the vortex height from the simulation has also been used.

The vortex model theory shown in Fig. 3 comes from using the expression for the fluid circulation, Γ , derived in Reference [3] (with values $P = 1.62$ Mbar, $\rho_H = 1.43$ g/cc, $\rho_L = 0.1$ g/cc, and $\gamma = 5/3$) in combination with the differential equations for the flow field

$$\frac{dx}{dt} = \frac{\Gamma}{4\lambda} \frac{\sinh\left(\frac{2\pi y}{\lambda}\right)}{\cos^2\left(\frac{\pi x}{\lambda}\right) + \sinh^2\left(\frac{\pi y}{\lambda}\right)} \quad (1)$$

$$\frac{dy}{dt} = \frac{\Gamma}{4\lambda} \frac{\sin\left(\frac{2\pi x}{\lambda}\right)}{\cos^2\left(\frac{\pi x}{\lambda}\right) + \sinh^2\left(\frac{\pi y}{\lambda}\right)}. \quad (2)$$

where a these differential equations imply vortex growth up to a saturation of the vortex amplitude to a value of $y_{max} = \cosh^{-1}(3)\lambda/2\pi \approx 0.281\lambda$ [3] the full vortex height then being $h_{max} = 2y_{max}$. Since Eqs. 1 and 2 trace out the trajectory that a massless particle would follow starting from some initial point (x_0, y_0) at $t = 0$, the full vortex height as plotted in Fig. 3 is then twice the value of the envelope of solutions to Eqs. 1 and 2 using the (x, y) locations that trace out the initial interface (see Fig. 4). An attempt to include the added complication of flow

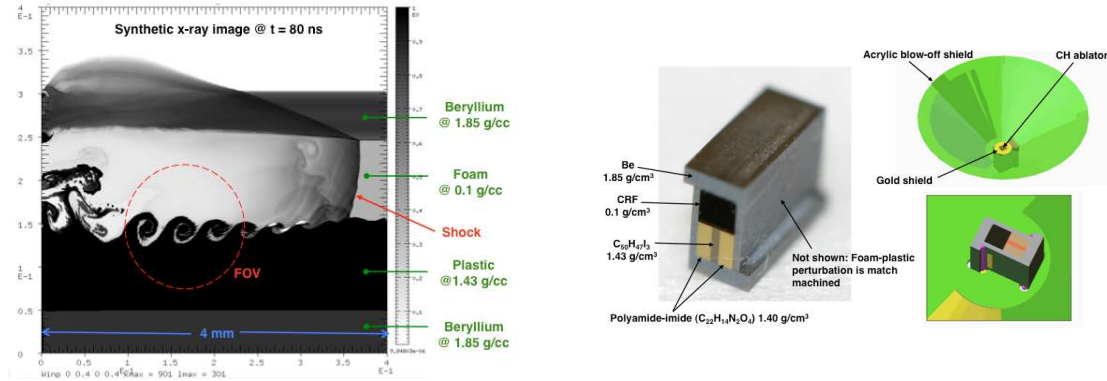


Figure 2. Left: A simulated radiograph result of a simulation of the target performance is shown at $t = 80$ ns. The materials that compose the target are annotated in the image. The field-of-view (FOV) accessible in the actual experiment is shown as the dashed red circle. Right: an annotated picture of the actual target. Note that the Be tube sides are $200 \mu\text{m}$ thick, while the top and bottom sections of the Be tube are $500 \mu\text{m}$ thick.

in the direction of vortex growth, due to the effect the transmitted shock, is shown in Fig. 3 as the stretched vortex model and is arrived at by adding a constant y -velocity of $2 \mu\text{m/ns}$ (from simulation) to the vortex model solution.

At late-time, the simulation and the stretched vortex model (which uses simulation derived values) both over predict the data. The simulation does exhibit the same change in growth rate at around $t = 38$ ns that the data shows. Inspection of the simulation at $t = 38$ ns indicates that this is the time at which the post-shock flow in the foam part of the target is arrested by the arrival of a rarefaction wave coming from the drive-side of the target.

The late-time over-prediction of the simulation is likely explained by the fact that the simulation is 2D, while the target itself is 3D. That is in 2D, the simulation the post-shock expansion of the shock-tube would under-estimate the real decay in the post-shock flow that results from the shock-tube expanding in 3D. Circumstantial evidence that supports this 3D shock-tube expansion hypothesis, is that the earlier 2D simulation [1] that uses a thinner Be shock-tube wall thickness than the simulation presented here is closer to the data at late time. An actually 3D simulation would be necessary to fully prove this hypothesis and some action in that direction is underway.

3. Bubbles in the free-stream

Bubbles located around the crests of the largest vortices at late-time (e.g. see the largest vortex of the rightmost frame of Fig. 1) in the data were unexpected. Several speculations about the origins of these bubble were put forth in the initial reports on these experiments [1, 2]. In spite of a strong superficial resemblance, further investigation of the trans-sonic shocklet [5] in the context of the present experiment now seems an unlikely explanation as the free-stream flow in the vicinity of the large vortices at late time is too low according simulations. Attempts to create a transonic effect in the simulations by assuming an ideal-gas equation of state and varying γ from $\gamma = 1.001$ to $\gamma = 6.0$ were also unsuccessful.

Cavitation-like behavior as an explanation for the observed bubbles is presently being investigated through the use of simulations that allow for multi-phase equations of state for the carbon foam used in the experiments. A more mundane effect that is related to the cavitation that occurs when an object penetrates from one fluid across and interface to another fluid [6] is presently the leading explanation for the bubble observed in the radiographs.

That is the simulation indicates that ablator plasma may be entrained into the free-stream

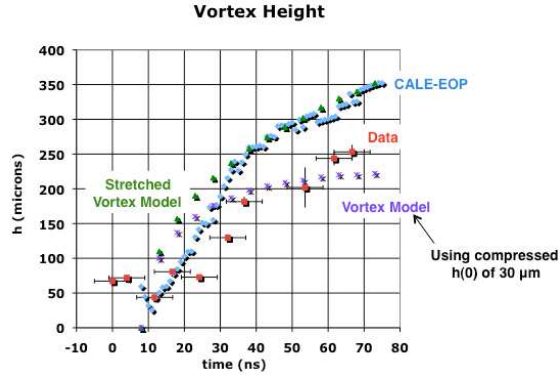


Figure 3. Vortex height versus time is shown for the experiment (red squares), the simulation (blue diamonds), and theory (purple asterisks and green triangles). The data and simulation both show a period of post-shock amplitude compression between 10 - 15 ns and subsequent amplitude growth. A distinct change in growth-rate is seen around 38 ns.

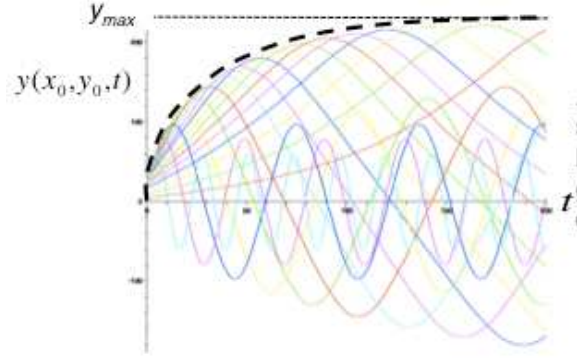


Figure 4. A family of solutions to the vortex model is shown and the envelope of these solutions is given by the dashed curve.

flow, due to the impulsive way in which this experiment is driven, and that the ablator material may be located in a bubble-like structure around the location of the largest vortex at 75 ns into the experiment. Moreover, as false-color simulated radiographs clearly show, the bubble of ablator material would have about 1/2 to 1/4 the optical depth of the surrounding post-shock carbon foam material. The morphology of the simulated bubble of ablator material is not, however, a perfect match to the observation but it is the closest simulated feature seen so far.

4. Conclusion

While some features seen in our HEDP KH experiment are yet to be fully explained, we have demonstrated the viability of the target design concept and demonstrated that high quality data on a KH unstable shear layer can be obtained. Simulation and theory are in fair agreement with the data obtained from this experiment with regard to the overall height of the vortex layer considering the fact that the simulation uses a simple laser source and lacks the 3D expansion of the shock tube.

In late 2009, we plan of fielding a follow-up set of HEDP KH experiments on the Omega laser that will examine the density scaling of the instability growth and simultaneously test the effect of the density on the development of the low density bubbles that appeared in the free-stream of the initial trials of this platform.

Further extensions of this platform to study multi-mode KH under HEDP conditions is easily accomplished by judicious choice of initial interface perturbation. Future experiments on NIF could create sustained steady flows with higher Reynolds numbers and use larger targets (for better diagnosis) both of which would enhance the usefulness of this platform.

Acknowledgments

This work has benefitted from the input of Dr.'s Andy Cook, Paul Dimotakis, George Langstaff, Aaron Miles, Paul Miller, Phil Sterne, Alan Wan, and Charlie Verdon. This work was performed under the auspices of the U.S. Department of Energy Lawrence Livermore National Laboratory

under contract No. DE-AC52-07NA27344. Work at the University of Michigan was sponsored by the National Nuclear Security Agency under the Stewardship Science Academic Alliances Program through DOE research grants DE-FG52-07NA28058, DE-FG52-04NA00064, and other grants and contracts.

- [1] O.A. Hurricane, J.F. Hansen, H.F. Robey, B.A. Remington, M.J. Bono, E.C. Harding, R.P. Drake, C.C. Kuranz, *Phys. Plasmas*, **16**, 056305, (2009).
- [2] E.C. Harding, J.F. Hansen, O.A. Hurricane, R.P. Drake, H.F. Robey, C.C. Kuranz, B.A. Remington, M.J. Bono, M.J. Grosskopf, R.S. Gillespie, *Phys. Rev. Lett.*, **103**, 045005, (2009).
- [3] O.A. Hurricane, High Energy Den. Phys., doi:10.1016/j.hedp.2008.02002, (2008).
- [4] R. T. Barton, "Development of a multimaterial two-dimensional, arbitrary Lagrangian-Eulerian mesh computer program," in *Numerical Astrophysics*, J.M. Centrella, J.M. LeBlanc, R.L. Bowers, eds., (Jones and Bartlett Publishers, Boston, 1985), p. 482.
- [5] P.E. Dimotakis, AIAA 91-1724, Proc. 22nd Fluid Dyn., Plasma Dyn., & Lasers Conf., (1991).
- [6] F. Ronald Young, "Cavitation," (Imperial College Press, London), 1999.